Appl. Phys. B 70, 695–700 (2000) / Digital Object Identifier (DOI) 10.1007/s003400000271

Applied Physics B
Lasers
and Optics

Dipole traps with mode-locked lasers

R.B.M. Clarke, T. Graf*, E. Riis

Department of Physics and Applied Physics, Strathclyde University, Glasgow, G4 0NG, Scotland, UK
(Fax: +44-0141/552-2891, Email: roger.clarke@strath.ac.uk)

Received: 30 September 1999/Revised version: 21 December 1999/Published online: 24 March 2000 –

Abstract. We investigate the properties of two separate dipole traps, realised using a cw mode-locked Ti:sapphire laser and a cw mode-locked Nd:YVO_4 laser, red-detuned by 25 nm and 284 nm, respectively. Approximately 10^3 laser-cooled ^{85}Rb atoms were confined in the traps at $\approx 50\,\mu$K, with no observable heating after initial loading. The lifetimes of the traps were consistent with limitations imposed by wavelength-dependent photoassociation losses and collisions with background vapour. Determination of the ac Stark shift of the 780 nm cooling transition using a weak probe beam showed no observable difference between using narrow-bandwidth or mode-locked trapping light. Techniques for trapping and focusing of atoms based on the dipole force of blue and uv light become much more accessible through efficient doubling, tripling and quadrupling of mode-locked sources. This opens up the possibility of manipulating more technologically interesting species.

PACS: 32.80.Pj; 32.80.Lg; 32.60.+i

Manipulation of laser-cooled atoms using the dipole force exerted by light has become a powerful tool in the repertoire of techniques available to the laser-cooling experimentalist [1–3]. The primary benefit of using the conservative dipole potential is that atoms may be trapped, guided or focused with virtually negligible scattering rates and correspondingly low heating rates [4–7] and long coherence times [8]. Laser-cooling applications include trapping of atoms [9] (including BECs [10]), guiding atoms along hollow optical fibres [11, 12], and focusing of atoms for atom lithography [7, 13–15]. Several geometries have been investigated, ranging from the simplest red-detuned focused laser beam [1] through to blue-detuned inverted pyramids [16] and atomic funnels [17].

To our knowledge all experiments to date have used single-frequency or narrow-band dipole light, but there are significant advantages of using cw mode-locked sources which have yet to be exploited, in particular when considering the possibilities for extending the range of atoms of interest beyond the alkali metals. Primarily, the high efficiencies of non-linear frequency conversion afforded by the very high peak powers available in short-pulse lasers extends the range of easily accessible high-power optical sources well into the blue and uv. For instance cw mode-locked light can be frequency doubled with efficiencies exceeding 40% in a single-pass configuration and $> 70\%$ in simple resonant enhancement cavities [18]. cw mode-locked lasers at $\approx 1\,\mu$m are readily available and can be frequency doubled or quadrupled [19] to obtain high-power sources of far-detuned light for technologically interesting species such as chromium, indium, silver and aluminium, which all have resonance transitions in the blue and uv part of the spectrum.

In this paper we demonstrate the trapping of laser-cooled ^{85}Rb atoms in two red-detuned dipole traps using two separate laser sources, both of which can be operated in mode-locked or narrow-band configurations. In both cases approximately 10^3 atoms were confined in the traps at $\approx 50\,\mu$K, with no observable heating after initial loading. In one case (using a Ti:sapphire laser tuned to about 805 nm) the lifetimes of the traps were consistent with limitations imposed by wavelength-dependent photoassociation losses [20], which is a problem that can be exacerbated by the wider bandwidth of the mode-locked source. In the other trap (using a Nd:YVO_4 laser at 1064 nm) the lifetimes for narrow-band and mode-locked operation were virtually identical and consistent with the limit imposed by the vacuum pressure. We probed the cooling transition at 780 nm and investigated its ac Stark shift to compare the properties of the dipole traps, both in mode-locked and narrow-band operation. A simple extension of conventional dipole trap theory allows one to calculate the properties of mode-locked dipole traps as a superposition of many single-frequency traps. For detunings larger than the mode-locked laser bandwidth the average trap depths and scattering rates are virtually identical to the single-frequency case with the same average power and detuning.

Compact solid-state cw mode-locked lasers at 1 μm typically have pulse lengths of a few ps, average powers of up to several W and repetition rates in the 100 MHz range. They

*Present address: Institute of Applied Physics, University of Bern, Sidlerstrasse 5, 3012 Bern, Switzerland

are commercially available and becoming increasingly reliable. For example, lasers using saturable Bragg reflectors (SBR) [24] are self-starting, can have high average power (≈ 10 W) and very short pulses ($<$ ps) and are extremely stable [25].

The output from a cw mode-locked laser is a train of coherent pulses repeating at the roundtrip time of the laser cavity. The spectrum of the laser is therefore a comb of modes separated by the free spectral range of the laser and spanning a bandwidth corresponding to the inverse of the duration of the individual pulses. The perfect coherence between the individual modes [22] and thereby successive pulses ensures that this type of laser is an ideal source for high-resolution laser spectroscopy [23]. The atomic response from the individual pulses add up coherently to yield a signal with a linewidth comparable to what would be obtained with a single-frequency source.

A notable difference between single-frequency and cw mode-locked operation of a dipole trap is encountered when considering the trap losses, particularly due to photoassociation [20]. When two trapped atoms collide the laser can excite a bound state in the 'molecular spectrum' formed by the long-range interaction potential of the atoms. In general this will lead to a significant amount of energy being transferred into kinetic energy and the two atoms are expelled from the trap. This is particularly a problem in the red-detuned trap where the atoms are confined to a high-intensity region. However, in the single-frequency case it can be avoided either by detuning far enough that the trapping laser is below the first excited state of the 'molecule' or by tuning in between two lines of the 'molecular spectrum' [20]. In the mode-locked case only the former works as the bandwidth of the laser far exceeds the line spacing.

The maximum instantaneous trap depth using a cw mode-locked laser is typically 2–5 orders of magnitude larger than when using a single-frequency laser of the same average power. However, as the atoms only experience the trapping potential for a correspondingly short fraction of the time, the force felt by the atom and averaged over a few pulses is the same in the two cases, and the most naive model for the trap would therefore suggest that the trajectories of atoms are identical. Indeed, this argument holds as long the repetition rate of the laser is much larger than the trap oscillation frequencies so that parametric oscillations are not driven. Most cw mode-locked lasers operating in the ps regime easily satisfy this condition as typical trap oscillation frequencies are of order a few tens of kHz. This intuitive temporal view of the trap works well, however, to calculate the trap properties it is much easier to consider the mode-locked light in frequency space where the single-frequency theory of dipole traps can be applied as a linear superposition.

1 Theory

We first review the ac Stark shift of an atomic level due to single-frequency light of detuning Δ and intensity I. The general expression for the potential energy, $\boldsymbol{U}$, of the ground state is given by [26]

$$\boldsymbol{U} = \frac{\hbar\Delta}{2}\ln(1+p)\,, \tag{1}$$

where p is the saturation parameter given by

$$p = \frac{I}{I_{\mathrm{Sat}}}\frac{\Gamma^2}{4\Delta^2+\Gamma^2}\,. \tag{2}$$

Γ is the linewidth of the transition and I_{Sat} is the saturation intensity of the transition. The scattering rate, $\boldsymbol{S}$, is given by [26]

$$\boldsymbol{S} = \Gamma\frac{p}{2(1+p)} \tag{3}$$

In the case of typical single-frequency dipole traps $p \ll 1$, such that $\ln(1+p)\approx p$, and $\Delta \gg \Gamma$, yielding the familiar result [9] that $\boldsymbol{U} = \hbar(I/I_{\mathrm{sat}})(\Gamma^2/8\Delta)$ and $\boldsymbol{S} = (I/I_{\mathrm{Sat}}(\Gamma^3/8\Delta^2)$. The trap depth expressed in Kelvin is given by $\hbar\Gamma^2/(12k_{\mathrm{B}}I_{\mathrm{Sat}})(I/\Delta)$. The counter-rotating term in the rotating wave approximation contributes an extra $\approx 15\%$ to the trap depth using the Nd:YVO_4 laser and less than 2% for the Ti:sapphire at 805 nm. These equations reduce to give a trap depth of $100I\,\mu$K for ^{85}Rb using a Nd^{3+} based laser ($\approx$1.06 μm) and $110I\,\mu$K for the Ti:sapphire laser at 805 nm, where I is expressed in units of mW/μm^2 and the 780-nm and 795-nm transitions have average saturation intensities of 2.4 and 4.8 mW/cm^2, respectively, for linearly polarised light. The corresponding scattering rates are $0.18I\,\mathrm{s}^{-1}$ and $31I\,\mathrm{s}^{-1}$, respectively.

The most straightforward analysis of trapping using a cw mode-locked laser is carried out in the frequency domain. We consider the output of the laser as a comb of modes separated by the free spectral range of the laser and spanning a bandwidth corresponding to the inverse of the duration of the individual pulses. We only consider the case where the bandwidth of the pulse is less than the detuning of the laser from resonance. The average scattering rate and trap depth due to the mode-locked light is then the sum of the average scattering rates and trap depths due to the individual modes, given by (3). This is justified by considering that each individual mode sets up an oscillating dipole moment in the atom. This mode can transfer energy to and from the atom over long time scales because the atom and the field oscillate at the same frequency. There is no contribution to the average energy transfer due to the other modes interacting with this dipole moment because the energy is transferred back and forth between the atom and the field at the beat frequency. Therefore the transfer of energy over long time scales can only be achieved by the interaction of the dipole moment with the mode that created it. We can therefore describe the interaction of the mode-locked laser with the atom as a sum of the independent contributions of the individual modes. This is valid as long as the total scattering rate obtained is much lower than saturation. For the Ti:sapphire and Nd:YVO_4 traps the excited state populations are $\approx 3.7\times10^{-6}$ and $\approx 8.0\times10^{-8}$, respectively, hence the approximation is valid. The trap depth calculations are performed in an analogous manner. For higher laser intensities and/or smaller detunings the interaction between the individual modes will have to be taken into account. This may be done more appropriately in the time domain, where the laser output is seen as a series of coherent pulses generally separated by less than the decay time of the atomic coherences.

We modeled the output of the Ti:sapphire laser used in the experiment as a series of sech^2 pulses with an average

detuning of 10 nm from the 795-nm line. The envelope function of the amplitude of the comb of modes is also a sech^2 function, yielding a time–bandwidth product of 0.315. For the 1-ps pulses used in the experiment the FWHM of the frequency comb is 0.68 nm. We sum the contributions of each mode to the scattering rate and include the variation of the detuning with each mode for both the 780-nm and 795-nm transitions. The calculated increase in the average scattering rates and trap depths are 0.27% and 0.072%, respectively, compared to the corresponding single-frequency case. We therefore conclude that there should be virtually no difference in the trap properties using mode-locked rather than single-frequency light in these typical operating conditions for the Ti:sapphire trap, other than photoassociation effects. With the Nd:YVO_4 trap the differences are completely negligible.

Table 1 gives a summary of the properties of the lasers used and the theoretical parameters of the dipole traps obtained using the effective single-frequency model.

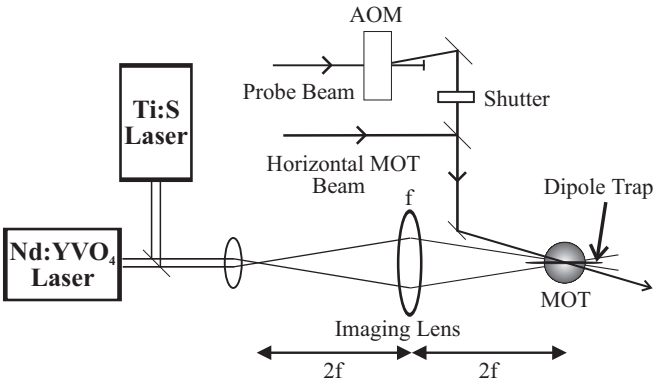

Figure 1

Fig. 1. The experimental arrangement based upon a conventional MOT and two separate cw mode-locked lasers. A frequency-tunable probe beam was used to measure the number of atoms in the trap and to scan the cooling transition

2 Experimental details

The experimental set-up was based upon a standard MOT which is described in more detail elsewhere [27]. A single-frequency Ti:sapphire laser provided the power for the cooling and probe beams, and a sideband injection-locked laser diode [28] was used as a repumper. Samples of $\approx 10^8$ atoms of ^{85}Rb were obtained in this system at a temperature of $\approx 20\,\mu$K.

A dipole trap was constructed with ≈ 300 mW of light from a tunable mode-locked Ti:sapphire laser with a repetition rate of 80 MHz and a pulse width of ≈ 1 ps. A tightly focused spot was imaged into the centre of the MOT using a $2f-2f$ relay lens arrangement, see Fig. 1. The 16.5-μm $1/e^2$ spot size radius was found by measuring the divergence of the light upon exiting the vacuum apparatus assuming a pure TEM_{00} beam. The light was typically detuned 10 nm to the red of the 795-nm transition to give a time-averaged trap depth of $\approx 770\,\mu$K.

The second mode-locked trap was constructed using a home-made Nd:YVO_4 laser with a saturable Bragg reflector (SBR) mirror to produce the mode-locking [25]. The small loss ($< 1\%$) in SBR mirror saturates at high peak powers, forcing the laser to mode-lock. This laser yielded an average power of 3.6 W at 1064 nm, of which 2.8 W was used in the dipole trap, yielding a time-averaged trap depth of $\approx 260\,\mu$K. The pulse widths were 33 ps. A flipper mirror was used to easily switch between the two dipole traps, enabling quick comparisons of the traps to be made and aiding alignment of the Nd:YVO_4 laser. Direct comparisons of the properties of traps in narrow-band and mode-locked operation could be made by replacing the SBR mirror with an ordinary high-reflection mirror. The power output was observed to be as stable as when in mode-locking operation. When the Ti:sapphire mode-locking mechanism was disrupted the laser output was a similar beam consisting of a number of simultaneously oscillating modes but with large power fluctuations ($\approx 5\%$) on timescales of order 30 kHz.

The dipole trap was loaded by focusing the dipole beam through the centre of the MOT whilst filling for 0.5 s, and then switching the cooling beams off. The repumping beam was left on for 2 ms longer to pump all the atoms into the $F=2$ ground state to eliminate losses due to spin-flip collisions. Approximately 10^3 atoms were held in the traps. The dipole light was kept on for a variable length of time before a tunable probe beam, resonant with the $F=3\rightarrow F=4$ cooling transition, and the repumping beam illuminated the trap. The probe beam was circularly polarised and was propagated along the axis of the dipole trap and retroreflected through a quarter-wave plate. This configuration leads to a linearly polarised standing wave (corkscrew) probe of constant intensity. The dipole light was on or off during this time to provide an easy comparison of the spectra of free space versus trapped atoms. The images of the dipole trap were captured on a CCD camera synchronised with the probe beam and the images analysed on an oscilloscope. For the experiments probing the cooling transition (see Sect. 3) the intensity and duration of the probe beam were chosen to be as small as possible ($0.2\,\mathrm{mW/cm^2}$ and 0.5 ms) whilst still maintaining a reasonable signal-to-noise ratio. This minimised trap loss due to heating when probing on the high-frequency side of the cooling transition.

Table 1. Properties of the two mode-locked lasers and the dipole traps constructed with them. The calculations are based on the spot sizes estimated by measuring the divergence of the dipole beam, assumed to be diffraction limited. The trap depth is given by the sum of the contributions to the $^5S_{1/2}$ state ac Stark shift due to the $^5P_{1/2}$ and $^5P_{3/2}$ states, using the theory described above. The counter-rotating term has been included in these calculations and the trap depths, scattering rates and phase changes per pulse are all peak values

	Ti:sapphire	Nd:YVO_4
Repetition rate, MHz	80	240
Mark-space ratio	12,500	130
Power, mW	300	2800
Spot size, μm	16.5	26.3
Wavelength, nm	805	1064
Δf S state ($P_{3/2}$), MHz	10.8	5.25
Δf S state ($P_{1/2}$), MHz	13.3	2.80
Trap depth, μK	770	260
Scattering rate, s^{-1}	22	0.47
Phase change per pulse, ϕ	$2\pi/2.8$	$2\pi/23$

The temperature of the atoms in the Nd:YVO_4 dipole trap was measured to be $\approx 50\,\mu$K by examining the ballistic expansion immediately after switching off the dipole light. During loading the atoms are spatially distributed throughout the trap, and thus have different potential energies, leading to large temperatures when the MOT light is switched off. Some boil-off quickly occurs leading to the more moderate temperature observed. There was no measurable increase in temperature of the atoms in the dipole trap from 100 ms up to at least 1000 ms – we studied the Nd:YVO_4 trap because its long lifetime permitted us to measure the heating rate for long times. Due to the falling cloud of untrapped atoms it was impossible to image the dipole trap reliably before 100 ms. Using the calculated trap properties given in Table 1, the trap volume corresponding to a depth of 50 μK is $\approx 1.6 \times 10^{-7}$ cm^3, with a length of approximately 2 mm. By comparing the fluorescence of dipole trap with the MOT we estimate that more than 1000 atoms are trapped, giving an average trap density of greater than 6×10^9 atoms cm^{-3}.

The trap lifetimes were determined by measuring the number of atoms remaining in the trap versus the time held in the traps. This was achieved by monitoring the fluorescence from the probe beam slightly red-detuned from the cooling transition. The Nd:YVO_4 traps in narrow-band and cw mode-locked operation had experimentally indistinguishable lifetimes of 2.0 ± 0.3 s, see Fig. 2, which is consistent with the loss due to the background vacuum pressure. The number of trapped atoms were also indistinguishable, demonstrating that mode-locked lasers can trap atoms as effectively as narrow-band lasers. The Ti:sapphire traps had lifetimes of 750 ms and 250 ms for narrow-band and cw mode-locked operation, respectively. The shorter lifetimes of these traps are consistent with the losses due to photoassociation present in the wavelength region used (800–825 nm), as described earlier. The mode-locked trap has a bandwidth of ≈ 0.68 nm and the average spacing between the photoassociation peaks at these wavelengths are approximately 0.5 nm [20]. The mode-locked trap therefore has a shorter lifetime than the corresponding narrow-band trap. By tuning the narrow-band trapping light it was possible to observe variations in the loss rates in a similar manner to Heinzen et al. The contribution to the lifetime of the traps due to scattering of the dipole light was negligible. The lifetime of the trap due to this scattering, $\tau = \boldsymbol{U}/2\boldsymbol{S}\boldsymbol{E}_{\mathrm{recoil}}$, is calculated to be 2200 s and 140 s for the Nd:YVO_4 and Ti:sapphire traps, respectively.

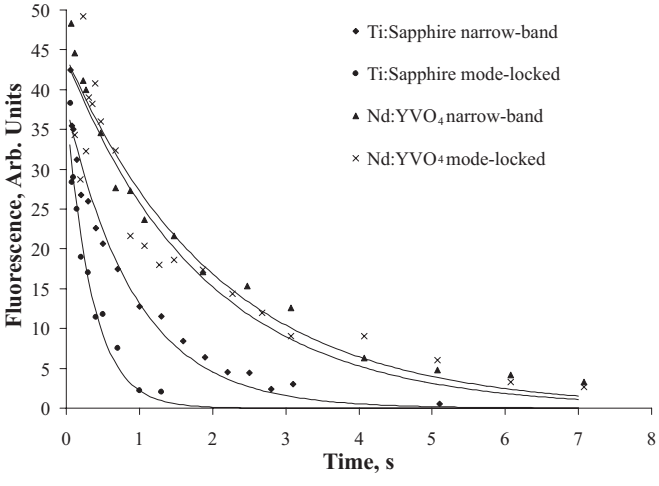

Fig. 2. Direct comparison of the lifetimes of the dipole traps in cw mode-locked and narrow-band operation. The Nd:YVO_4 traps had experimentally identical lifetimes of 2.0 s, limited by background vacuum pressure, demonstrating that mode-locked light can trap atoms as effectively as narrow-band sources. The lifetimes of the Ti:sapphire traps operating at 805 nm were lower due to photoassociation losses, particularly in the mode-locked configuration as a result of the large bandwidth (≈ 1 nm) of the light covering many photoassociation lines. The solid lines are least-square fits to a single exponential and the experimental values had errors of approximately 10%

3 ac Stark shift

In a single-frequency trap the ac Stark shift can be regarded as a shift in the oscillation frequency of the dipole moment of the atoms, or equivalently as a continual phase advance of slippage compared to unperturbed atoms, see Fig. 3. In the case of a cw mode-locked trap with the same average power as a single-frequency trap, the phase change is compressed into the duration of the pulses where the dipole moment rotates at a different rate. Assuming a large MSR, the phase change per pulse ϕ is then simply the phase change that would have accumulated during the time between consecutive pulses, and is given by $\phi = 2\pi\delta/R$ where δ is the ac Stark shift of the equivalent single-frequency trap of the same average intensity, and R is the repetition rate of the pulses. We also assume that the total scattering rate is small. If $\phi \ll 2\pi$ and the repetition rate of the laser is greater than Γ (so that there are many pulses per decay lifetime), the observed ac Stark shift is identical to that in the single-frequency case as the series of small phase shifts approximate to a smooth change over the excitation time. This was confirmed by simulating the absorption spectrum of an atomic line in such a pulsed field using a frame rotation in which the dipole moment of the atom evolves continuously and the driving electric field evolves with appropriate phase changes at the repetition rate. Taking the Fourier transform of this light with the exponential decay of the atom yields the absorption spectrum, which was identical to continuous single frequency driving light for

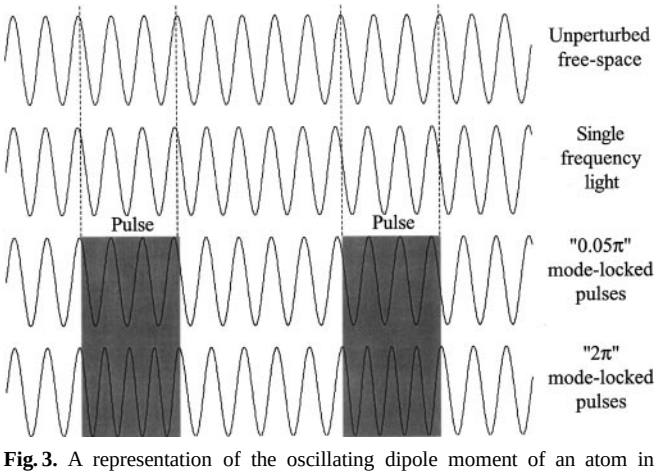

Fig. 3. A representation of the oscillating dipole moment of an atom in free space, in a single-frequency dipole beam and two cw mode-locked dipole beams where $\phi = 0.05\pi$ and $\phi = 2\pi$. In this figure the single-frequency dipole beam and the 0.05π mode-locked dipole beam have the same average intensities but the phase of the atomic dipole moment evolves differently, demonstrating the compression of the phase shift into the pulses

the parameters used in both experimental traps. By increasing the intensity and/or decreasing the detuning and the repetition rate, it is possible to make $\phi = 2n\pi$, where n is an integer. In this instance the trap potential still remains, because the ac Stark shift is present during the pulses, however the *observed* position of the cooling transition is unshifted because the resultant phase of the dipole moment is unaffected by each pulse. We therefore predict a wrap-around effect at $\pm R/2$ in the position of the observed cooling transition as ϕ increases.

The observed frequency shift of the transition is given by the sum of the ac Stark shifts of the $S_{1/2}$ manifold and the individual $P_{3/2}$ states that are being probed. The levels in the $S_{1/2}$ manifold all shift by the same amount because Δ is much greater than any of the energy splittings within the manifold and the combined contributions to the ac Stark shift from all the hyperfine levels in each P state add to give the same total shift. However, each individual m_F state in each P manifold experiences a shift that depends on the oscillator strengths of the transitions to the S state levels. Therefore the observed ac Stark shift is dependent on the upper state of the transition being probed. We assume an even distribution in the ground m_F levels since the atoms can be in all possible states after being in the MOT. For the Nd:YVO_4 trap the average contribution to the observed shift due to the P states is $5.25\,\mathrm{MHz} \times 0.77$. The measured temperature of $\approx 50\,\mu\mathrm{K}$ leads to a reduction in the average ac Stark shift of $\approx 13\%$, leading to a total expected shift of 10.5 MHz. Experimentally the shift was found to be ≈ 5 MHz, see Fig. 4, and we observed the same shift to within experimental error when we switched to narrow-band operation of the Nd:YVO_4 laser. There was therefore no observable difference in trap behaviour between mode-locked and narrow-band dipole traps in this regime.

Estimating the spot size by measuring the beam divergence would tend to overestimate the intensity as the beam profile is affected by spherical aberration in the relay lens (a bi-convex lens with a focal length of 25 cm and a diameter of 2.7 cm) as well as any deviation from a perfect TEM_{00} laser mode and distortions of the beam along the optical path. We are not aware of a full Gaussian treatment of the spherical aberration problem, but by using an expression for the third-order spherical aberration [21] we can calculate the variation in the classical focal length over the $1/e^2$ intensity radius (≈ 1 cm on the lens) to be ≈ 2 mm. If a TEM_{00} beam with a divergence of 19 mrad (as observed with the Nd:YVO_4 laser) is defocused by 2 mm the beam cross-sectional area more than doubles. This suggests that a significant part of the difference between observed and expected ac Stark shifts is due to spherical aberration from the relay lens.

The experimental scans of the Ti:sapphire trap were not wide enough to observe a feature at the predicted shift of 28.2 MHz, given by the same methodology as in the Nd:YVO_4 trap, but we did detect a broad feature shifted by ≈ 2.5 MHz from the unperturbed line. Again, there was no experimentally observable difference in the scans when narrow-band Ti:sapphire light was used.

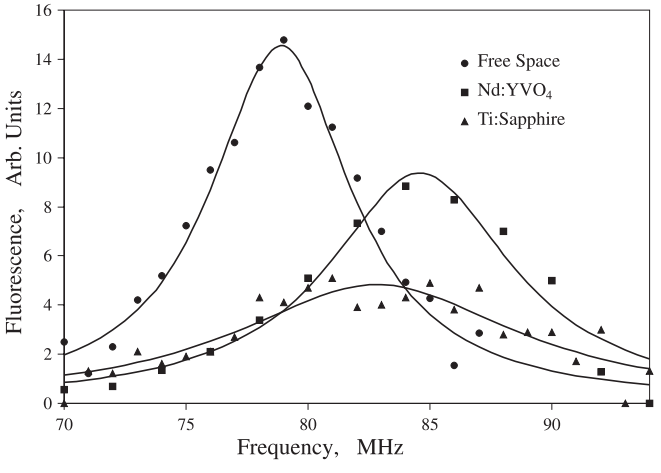

Fig. 4. Frequency scans of the cooling transition whilst the Nd:YVO_4 and Ti:sapphire cw mode-locked traps were on, and with the atoms in free space. An AOM was used to scan the probe beam. The shift of the transition in the cw mode-locked Nd:YVO_4 trap is smaller than the theoretical predictions but identical to the shift observed using the laser in narrow-band operation. The predicted observable shift of the Ti:sapphire trap is 28.2 MHz, outside of the range of the scan, but a broad, weak feature is still observed. The feature does not change when the mode-locking mechanism is disrupted to give narrow-band light

4 Conclusions

We have demonstrated two separate dipole traps constructed using both cw mode-locked and narrow-band laser light. The lifetimes of the traps were measured and consistent with the frequency properties of the dipole light. Spectroscopy of the cooling transition demonstrated that there was no observable difference between cw mode-locked and narrow-band lasers in the regimes used. We conclude that mode-locked dipole beams can be used to open the doorway for trapping and focusing more technologically interesting species using efficient non-linear frequency conversion of mode-locked laser sources.

Acknowledgements. This work was supported by the UK Engineering and Physical Sciences Research Council (EPSRC). We wish to thank C.S. Adams and D.H. McIntyre for their help and useful discussions, and A.I. Ferguson for the use of the Nd:YVO_4 laser.

References

1. S. Chu, J.E. Bjorkholm, A. Askin, A. Cable: Phys. Rev. Lett. **59**, 314 (1986)
2. C.I. Westbrook, R.N. Watts, C.E. Tanner, S.L. Rolston, W.D. Phillips, P.D. Lett: Phys. Rev. Lett. **65**, 33 (1990)
3. A. Kastberg, W.D. Phillips, S.L. Rolston, R.J.C. Spreeuw, P.S. Jessen: Phys. Rev. Lett. **74**, 1542 (1995)
4. T. Takekoshi, R.J. Knize: Opt. Lett. **21**, 77 (1996)
5. C. Salomon, J. Dalibard, A. Aspect, H. Metcalf, C. Cohen-Tannoudji: Phys. Rev. Lett. **59**, 1659 (1987)
6. J.E. Bjorkholm, R.R. Freeman, A. Ashkin, D.B. Pearson: Phys. Rev. Lett. **41**, 1361 (1978)
7. B. Brezger, T. Schulze, U. Drodofsky, J. Stuhler, S. Nowak, T. Pfau, J. Mlynek: J. Vac. Sci. Technol. B **15**, 2905 (1997)
8. N. Davidson, H.J. Lee, C.S. Adams, M. Kasevich, S. Chu: Phys. Rev. Lett. **74**, 1311 (1995)
9. J.D. Miller, R.A. Cline, D.J. Heinzen: Phys. Rev. A **47**, 4567 (1993)
10. J. Stenger, D.M. Stamperkurn, M.R. Andrews, A.P. Chikkatur, S. Inouye, H.J. Miesner, W. Ketterle,: J. Low Temp. Phys. **113**, 167 (1998)
11. H. Ito, K. Sakaki, W. Jhe, M. Ohtsu: Opt. Commun. **141**, 43 (1997)
12. J.P. Yin, Y.F. Zhu, Y.Z. Wang: Phys. Rev. A **57**, 1957 (1998)

13. G. Timp, R.E. Behringer, D.M. Tennant, J.E. Cunningham, M. Prentiss, K.K. Berggren: Phys. Rev. Lett. **69**, 1636 (1992)
14. J.H. Thywissen, K.S. Johnson, R. Younkin, N.H. Dekker, K.K. Berggren, A.P. Chu, M. Prentiss, S.A. Lee: J. Vac. Sci. Technol. B **15**, 2093 (1997)
15. H. Chen, E. Riis: Appl. Phys. B **69**, 10 (2000)
16. C.S. Adams, H.J. Lee, N. Davidson, S. Chu: Phys. Rev. Lett. **74**, 3577 (1995)
17. O. Morsch, D.R. Meacher: Opt. Commun. **148**, 49 (1998)
18. A.S. Bell, E. Riis, A.I. Ferguson: Opt. Lett. **22**, 531 (1997)
19. G.P.A. Malcolm, M.A. Persaud, A.I. Ferguson: Opt. Lett. **16**, 983 (1991)
20. J.D. Miller, R.A. Cline, D.J. Heinzen: Phys. Rev. Lett. **71**, 2204 (1993)
21. F.A. Jenkins, H.E. White: *Fundamentals of Optics*, 4th edn. (McGraw-Hill, London 1985) p.157
22. T. Udem, J. Reichert, R. Holzwarth, T.W. Hänsch: Opt. Lett. **24**, 881 (1999)
23. M.J. Snadden, R.B.M. Clarke, E. Riis: Opt. Commun. **152**, 283 (1998)
24. U. Keller, K.J. Weingarten, F.X. Kärtner, D. Kopf, B. Braun, I.D. Jung, R. Fluck, C. Hönninger, M. Matuschek, J. Aus der Au: IEEE J. Sel. Top. Quantum Electron. **2**, 435 (1996)
25. Th. Graf, A.I. Ferguson, E. Bente, D. Burns, M.D. Dawson: Opt. Commun. **159**, 84 (1999)
26. A. Ashkin: Phys. Rev. Lett. **40**, 729 (1978)
27. A.G. Sinclair, E. Riis: Opt. Commun. **119**, 527 (1995)
28. M.J. Snadden, R.B.M. Clarke, E. Riis: Opt. Lett. **22**, 892 (1997)